Available online at www.sciencedirect.com

ScienceDirect

Scripta Materialia 88 (2014) 29–32

Scripta MATERIALIA

www.elsevier.com/locate/scriptamat

Initial dynamics of a solid–liquid interface within a thermal gradient

M. Xu,[a] L.M. Fabietti,[b,c] Y. Song,[d] D. Tourret,[d] A. Karma[d] and R. Trivedi[a,*]

[a]*Department of Materials Science and Engineering, Iowa State University, Ames, IA 50011, USA*
[b]*Facultad de Matemática Astronomía y Física, Universidad Nacional de Córdoba, Argentina*
[c]*Instituto de Fisica Enrique Gaviola, Conicet, Cordoba, Argentina*
[d]*Department of Physics and Center for Interdisciplinary Research on Complex Systems, Northeastern University, Boston, MA 02115, USA*

Received 17 October 2013; revised 5 June 2014; accepted 6 June 2014
Available online 19 June 2014

In directional solidification experiments an alloy is placed in the thermal gradient assembly and kept stationary to achieve a steady-state thermal profile. During this time an interface motion occurs that is experimentally characterized and shown to generate a solute boundary layer at the interface whose thickness depends on the time the sample is kept stationary before the external velocity is imposed. This boundary layer must be included in the theoretical description of the initial transient during a planar front growth.

Keywords: Directional solidification; Interface dynamics; Bridgman technique; Crystal growth; Boundary layer

The dynamics of solid–liquid interfaces plays a crucial role in the evolution of microstructures during directional solidification of alloys. The most basic process is the motion of a planar interface in a binary alloy system that is controlled by the development of a solute boundary layer with time until a steady-state condition is reached. Theoretical models have been proposed by using approximate analytical treatments or numerical simulations [1–6]. In all the models proposed so far, the sample is considered to solidify from one end so that the initial composition in the liquid is uniform. In contrast, in directional solidification experiments, a solid alloy of uniform composition is placed in a thermal gradient stage. The sample is generally held stationary until a steady-state thermal profile is established and a planar interface forms [7]. The sample is then moved at a fixed rate to achieve directional solidification.

When the sample is placed in the thermal gradient stage (Fig. 1a) the liquid and solid are at the initial alloy composition far from the interface, but the liquid and solid compositions at the interface must be different for local equilibrium to be present. Therefore, solute boundary layers develop, as schematized in Figure 1b, which in turn influence the concentration field when the sample is directionally solidified, and must be taken into account in the description of the initial transient during the planar front growth.

Nguyen Thi et al. [8] first characterized the presence of an initial solute boundary layer in an Al–1.5 wt.% Ni alloy. They discussed the homogenization process by temperature gradient zone melting process in the mushy zone, and concluded that when liquid diffusion is the mode of transport, the limiting condition of a homogeneous liquid may not be fulfilled due to the very long time required.

The present study examines the dynamics of the planar interface that forms quickly in a dilute alloy of a transparent system in the presence of a thermal gradient but no externally imposed velocity. We seek to determine the position or temperature of the interface when the interface stabilizes and remains stationary within the temperature gradient. For a pure material the interface will be at the melting point isotherm. However, in a binary system the interface temperature can have any value between

* Corresponding author; e-mail addresses: rohit.k.trivedi@gmail.com; trivedi@iastate.edu

http://dx.doi.org/10.1016/j.scriptamat.2014.06.006
1359-6462/

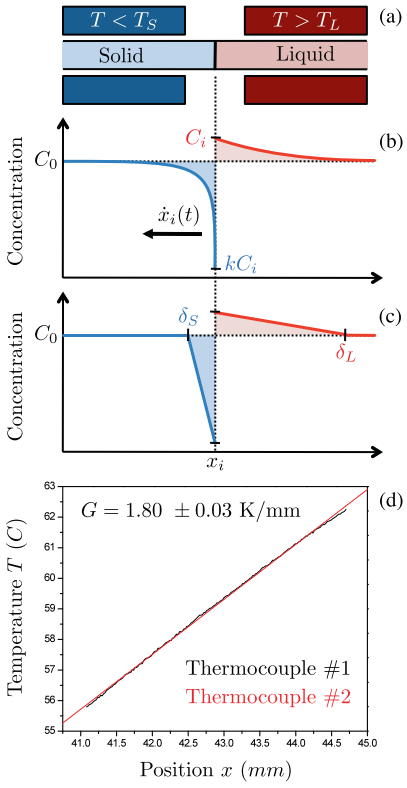

Figure 1. (a) Experimental setup in which a solid of initial uniform composition, C_0, is placed in the thermal gradient stage with zero imposed velocity. Composition profiles develop in the solid and liquid to maintain local equilibrium at the interface while the interface recoils, as illustrated in the schematic snapshot in (b) with boundary layer equivalent profiles in (c). The temperature profiles obtained from two thermocouples, shown in (d), overlap when relatively displaced by the distance between the thermocouples, hence confirming a homogeneous thermal gradient $G = 1.8$ °C mm^{-1}.

the liquidus and the solidus temperatures, and the interface must stabilize between these two temperatures.

Experiments were carried out with succinonitrile (SCN)–0.25 wt.% camphor. As-received SCN was first purified by distillation and a zone-refining process. Camphor with initial purity of 98 wt.% was sublimated twice at a temperature of 353 K under vacuum of 45 Pa. High-purity SCN was then mixed with a camphor in a glovebox filled with an inert environment of nitrogen to obtain the SCN–0.25 wt.% camphor mixture. The liquid alloy was introduced into the sample cell and cooled quickly to obtain a solid sample of fine microstructure that consisted of equiaxed dendrites and eutectic. A rectangular sample 100 μm thick was used to minimize convection in the liquid. Two additional cells, identical to the sample cell, were also prepared, and calibrated thermocouples were placed in these two cells. The cells with thermocouples were placed on the two sides of the sample cell, and the three-cell assembly was placed in the temperature gradient stage. The hot and cold baths were maintained at 73 and 48 °C, respectively, yielding a nominal thermal gradient of 1.8 °C mm^{-1}.

The thermocouples in the outer cells were placed at a fixed distance from each other in the growth direction, such that the solid–liquid interface in the center sample was present between these two thermocouples. First the sample assembly was directionally solidified at a fixed growth rate, and the temperature profiles given by the two thermocouples were characterized. When displaced by the distance between the thermocouples, the temperature profiles from the two thermocouples overlapped, as shown in Figure 1d, hence confirming the presence of steady-state thermal field. The temperature gradient measured in the region between the two thermocouples was 1.8 °C mm^{-1}, identical to a direct calculation from the measured temperature at the two thermocouples divided by the distance between them, hence confirming a linear temperature profile in the sample near the interface.

The temperature profiles are linear and continuous through the solid–liquid interface since the thermal conductivities of solid and liquid SCN are nearly equal, at 0.225 and 0.223 W K^{-1} m^{-1}, respectively [9]. Thus, the interface temperature can be calculated at any time from the thermal gradient value and the location of the interface.

A fresh sample cell was prepared and placed in the thermal gradient for quantitative measurements of interface position with time with no imposed velocity. Once the sample was placed in the thermal gradient stage, melting in the hot zone occurred rapidly above the liquidus temperature and a planar solid–liquid interface formed. Since the sample is held stationary the thermocouple positions remain fixed and only the interface position changes with time. The evolution of the interface location was measured from a fixed reference position, which was taken as the sharp edge of the cold chamber. The initial position of the interface was then taken as $x = 0$, and the positive x direction was taken towards the cold stage. The measured position of the interface with time, $x_i(t)$, appears in Figure 2.

Given the constant temperature gradient, the variation of interface temperature with time is calculated, as shown on the right hand side of Figure 2. From the expression given by Teng and Liu [10], the liquidus temperature for the alloy of composition $C_0 = 0.25$ wt.% camphor is $T_L = 57.73$ °C. The solidus temperature at C_0 measured as the interface temperature during steady-state planar interface growth is $T_S = 56.45$ °C. Hence, assuming linear liquidus and solidus lines from the melting temperature of pure SCN, T_M, with $T_L = 57.73$ °C and $T_S = 56.45$ °C, and using a solute partition coefficient, $k = 0.21$ [10], the liquidus line of the alloy follows $T = T_M + mC_i$ with $T_M = 58.07$ °C and a liquidus slope $m = -1.361$ °C wt.%$^{-1}$. Therefore, we can plot the

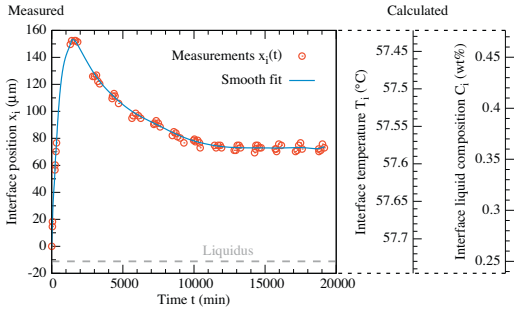

Figure 2. Experimental measurement of the time evolution of interface position $x_i(t)$ (left y-axis) and corresponding calculated evolution of the interface temperature and liquid interface composition (right axes).

variation of the interface composition in the liquid, as shown on the right-hand side of Figure 2.

First, the interface moves towards the cold stage so that the interface temperature decreases with time. The interface temperature goes through a minimum at ≈ 57.43 °C (i.e. an interface composition maximum of ≈0.47 wt% camphor). Then the direction of the interface motion changes, moving towards the hot stage with decreasing rate until the interface approaches a fixed position. The final stationary position of the interface is at a temperature 57.58 °C. Since the freezing range of the alloy is $\Delta T_0 = T_L - T_S = 1.28$ °C, the final interface undercooling is $\Delta T = 0.15$ °, i.e. a dimensionless undercooling $\Delta T/\Delta T_0 = 0.117$, and a final liquid interface composition of 0.36 wt% camphor.

Hence, the solid first melts and then solidification occurs until the interface velocity slowly approaches zero. Initially when the sample is placed in the thermal gradient stage, a small region of two-phase structure is observed behind the interface in the solid matrix that contains droplets of liquid. These droplets migrate towards the interface due to temperature gradient zone melting [8]. The liquid bubbles of high solute concentration get incorporated into the liquid at the interface, hence causing the liquid interface composition to increase and the interface to melt. When all the droplets are removed, the liquid interface composition is maximum, and then decreases until a constant interface composition is reached.

One important observations is that when the interface is not subject to an externally imposed velocity it approaches a stationary position after a long time at which point the velocity of the interface approaches zero and the interface stabilizes at a temperature below the alloy liquidus. In our experiment, the interface velocity approaches zero after 14 days. This is not an equilibrium condition since that would require constant compositions in the liquid and in the solid, or more accurately constant chemical potential of the solute in the system since the temperature is not homogeneous. Global equilibrium will not occur due to kinetic limitations because of the slow diffusion in solid.

To estimate the dynamics of the interface in a purely diffusive regime, we solve numerically the one-dimensional sharp-interface problem of two equations controlling the dynamics of the interface, namely the diffusion equation in the bulk phases:

$$\frac{\partial C}{\partial t} = D\frac{\partial^2 C}{\partial x^2}, \tag{1}$$

and the Stefan's condition, i.e. the flux balance at the interface:

$$(1-k)C_i\dot{x}_i(t) = D_S\left.\frac{\partial C}{\partial x}\right|_S - D_L\left.\frac{\partial C}{\partial x}\right|_L, \tag{2}$$

where D_S and D_L are the solute diffusion coefficients in the solid and liquid, respectively, $x_i(t)$ is the position of the interface with its time derivative $\dot{x}_i(t)$, and the subscript S (L) in the right-hand side of Stefan's condition stands for the composition gradient on the solid (liquid) side of the interface at $x = x_i(t)$. For numerical convenience, we apply the change of variable $y \equiv x/x_i(t)$, such that the constitutive equations of the model become:

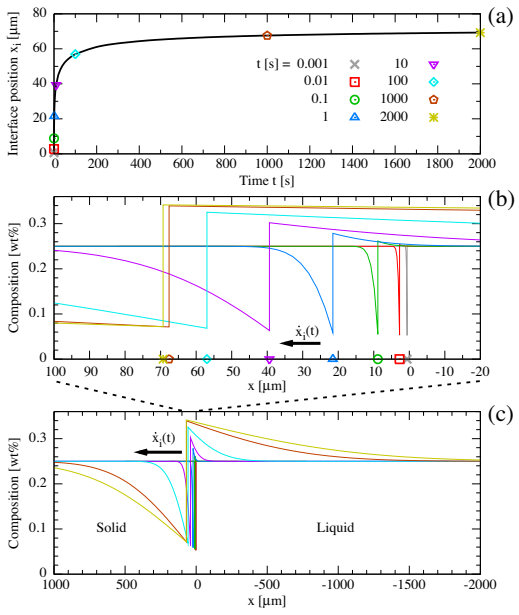

Figure 3. Calculated evolution of the solid–liquid interface position $x_i(t)$ (a) and solute composition profiles (b,c) as predicted by a sharp-interface 1-D diffusion model, i.e. Eqs. (1) and (2), with $k = 0.21$, $D_L = 2.4\ 10^{-10}$ $m^2\ s^{-1}$ and $D_S/D_L = 0.3$. Snapshot symbols in (a) correspond to the composition profile snapshots represented at the scale of the interface motion in (b) and at the much larger scale of diffusion in (c), with similar symbols marking the interface position $x_i(t)$ on the bottom axis of (b).

$$\frac{\partial C}{\partial t} = \frac{D}{x_i(t)^2}\frac{\partial^2 C}{\partial y^2} + y\frac{\dot{x}_i(t)}{x_i(t)}\frac{\partial C}{\partial y} \tag{3}$$

$$(1-k)C_i\dot{x}_i(t) = \frac{D_S}{x_i(t)}\left.\frac{\partial C}{\partial y}\right|_S - \frac{D_L}{x_i(t)}\left.\frac{\partial C}{\partial y}\right|_L. \tag{4}$$

We solve these two equations numerically using finite differences and an explicit Euler time scheme. Figure 3 shows the results of the model for $C_i = 0.25$ wt.%, $k = 0.21$, a liquid diffusivity $D_L = 2.4\ 10^{-10}$ $m^2\ s^{-1}$ [10], an illustrative solid diffusivity $D_S = 0.3\ D_L$, and a temperature gradient of 1.8 °C mm^{-1}. These calculations do not account for the presence of the two-phase region with high-concentration liquid bubbles, and therefore do not predict the maximum recoil value seen experimentally. However, Figure 3a shows the steep initial slope of $x_i(t)$, and the interface quickly stabilizes to a fixed position, even though composition profiles on both sides of the interface are still evolving toward a complete equilibrium at much longer time and length scales, as seen in Figure 3b (close to the interface) and Figure 3c (at a larger length scale). These results show that only when diffusion in the two phases is considered, a finite amount of initial undercooling is present at the interface that is associated with a solute boundary layer in the liquid.

We now examine the factors that determine the magnitude of the interface undercooling when the interface velocity approaches zero for a stationary sample. In a semi-infinite phase, the 1-D moving boundary problem admits a well-known analytical solution (e.g. Appendix 1 in Ref. [9]) that appears by taking $x = 0$ at the interface and combining x and t into $z = x(Dt)^{-1/2}$, hence changing the diffusion Eq. (1) to:

$$\frac{\partial^2 C}{\partial z^2} + \frac{z}{2}\frac{\partial C}{\partial t} = 0, \tag{5}$$

integration of which yields the similarity solution for the composition profile:

$$C(x,t) = C^* + (C^0 - C^*)\mathrm{erf}\left(\frac{x}{\sqrt{4Dt}}\right) \tag{6}$$

with

$$\mathrm{erf}(z) = \frac{2}{\sqrt{\pi}}\int_0^z \exp(-u^2)\,\mathrm{d}u, \tag{7}$$

and the integration constants identified through the boundary conditions $C(0,t) = C^*$ at the interface and $C(\infty, t) = C_0$ far away in the bulk. These composition profiles are present in both phases with $C^* = C_i$ in the liquid and $C^* = kC_i$ in the solid, if x is the distance to the interface. Given the error function composition profiles in both phases, we can introduce the diffusion lengths in the solid δ_S and in the liquid δ_L, as illustrated in Figure 1c, and write the flux balance at the interface (2) with $\dot{x}_i(t) = 0$ as:

$$D_S\frac{kC_i - C_0}{\delta_S} - D_L\frac{C_0 - C_i}{\delta_L} = 0. \tag{8}$$

By defining the diffusivities ratio $\alpha = D_S/D_L$, the flux balance at the interface yields:

$$\alpha = \frac{(C_i - C_0)}{(C_0 - kC_i)}\frac{\delta_S}{\delta_L}. \tag{9}$$

In addition to the interfacial flux balance, one must also satisfy the total solute mass balance of the system that requires that the depletion of solute in the solid be equal to the build-up of solute in the liquid, which can be written as:

$$(\mathrm{C_i} - C_0)(\delta_L) = (C_0 - kC_i)(\delta_S). \tag{10}$$

Substituting the resulting value of δ_S/δ_L into the interface flux balance one obtains:

$$\frac{C_\mathrm{i}}{\mathrm{C_0}} = \frac{1 + (\alpha)^{1/2}}{1 + \mathrm{k}(\alpha)^{1/2}}. \tag{11}$$

This result, which can be identically obtained using the exact error function profiles, shows that the composition at the interface when the interface velocity approaches zero depends on the ratio of the diffusivities in the solid and the liquid.

We now consider the limiting cases. For zero diffusion in the solid, i.e. $\alpha = 0$, $C_i = C_0$ and the interface is at the liquidus temperature; for $\alpha \to \infty$, $C_i = C_0/k$ and the planar interface is at the solidus temperature. Thus the stationary interface temperature will vary from the liquidus to the solidus temperature as the ratio of diffusivities varies from zero to infinity. This is confirmed by the simulation results in Figure 4, where we show the time evolution of the interface for different values of the diffusivity ratio. Since $D_S = \infty$ is not realistic, the largest value of D_S is considered to be D_L, so that $\alpha = 1$ and thus $C_i \to [2/(1+k)]C_0$. Additionally, by measuring the recoil of the planar interface, this analysis can yield a valuable estimate of the diffusivity ratio, e.g. here $\alpha \approx 0.3$ since the recoil measured experimentally is ~70 μm (see Figs. 2 and 4). Note that this value of the ratio is overestimated since the presence of the two-phase region in the solid is not considered in the model.

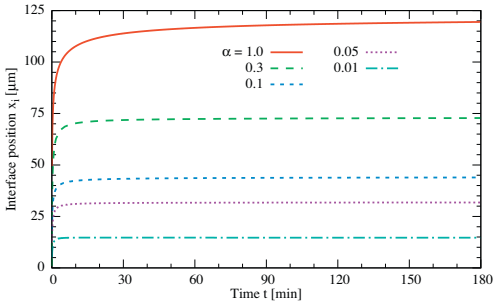

Figure 4. Predictions of the solid–liquid interface position evolution $x_i(t)$ calculated by the sharp-interface model for different values of the diffusivity ratio $\alpha = D_S/D_L$.

We have established the presence of solute boundary layers while an alloy sample is kept stationary in the thermal gradient zone. The diffusion dynamics are very slow, so that a very long time would be required to approach constant interface compositions. The presence of solute boundary layers before the sample is moved will significantly influence the subsequent solute build-up dynamics when a planar interface growth is initiated by moving sample, as shown recently by Fabietti et al. [11]. To determine the precise interface transient dynamics after the sample translation is initiated, one needs to characterize the initial solute boundary layer. While this is not important to obtain a zero interface velocity, which may take a very long time, it is critical to measure the interface temperature at the start of the directional solidification in order to estimate the initial composition profile in front of the interface and use it as initial condition for the analysis of directional solidification when the sample is translated with respect to the thermal gradient. Simple measurements of interface position vs. time are not sufficient since they do not provide any information on the extent of the initial boundary layer present.

This research was supported by NASA Grant No. NNX12AK54G.

[1] W.A. Tiller, K.A. Jackson, J.W. Rutter, B. Chalmers, Acta Metall. 1 (1953) 428.
[2] V.G. Smith, W.A. Tiller, J.W. Rutter, Can. J. Phys. 33 (1953) 723.
[3] J.C. Clayton, M.C. Davidson, D.C. Gillies, S.L. Lehoczky, J. Cryst. Growth 60 (1982) 374.
[4] B. Caroli, C. Caroli, L. Ramirez-Piscina, J. Cryst. Growth 132 (1993) 377.
[5] S.R. Coriell, R.F. Boisvert, G.B. McFadden, L.N. Brush, J.J. Favier, J. Cryst. Growth 140 (1994) 139.
[6] J.A. Warren, J.S. Langer, Phys. Rev. E 47 (1993) 2702.
[7] K. Sombooksun, J.T. Mason, R. Trivedi, Metall. Mater. Trans. A 15 (1984) 967.
[8] H. Nguyen Thi, B. Drevet, J.-M. Debierre, D. Camel, Y. Dabo, B. Billia, J. Cryst. Growth 253 (2003) 539.
[9] W. Kurz, D.J. Fisher, Fundamentals of Solidification, third ed., TransTech, Aedermannsdorf, 1992.
[10] J. Teng, S. Liu, J. Cryst. Growth 290 (2006) 248.
[11] L.M. Fabietti, M. Xu, P. Mazumder, R. Trivedi, Unpublished work, Iowa State University, 2013.